A survey of greenhouse gases production in central European lignites

Anna Pytlak, Anna Szafranek-Nakonieczna, Weronika Goraj, Izabela Śnieżyńska, Aleksandra Krążała, Artur Banach, Ivica Ristović, Mirosław Słowakiewicz, Zofia Stępniewska

A survey of greenhouse gases production in central European lignites

Anna Pytlak [a,*], Anna Szafranek-Nakonieczna [b], Weronika Goraj [b], Izabela Śnieżyńska [c], Aleksandra Krążała [c], Artur Banach [b], Ivica Ristović [d], Mirosław Słowakiewicz [c,e], Zofia Stępniewska [f]

[a] Institute of Agrophysics, Polish Academy of Sciences, ul. Doświadczalna 4, 20-290 Lublin, Poland
[b] Institute of Biological Sciences, The John Paul II Catholic University of Lublin, Konstantynów 1 I, 20-708 Lublin, Poland
[c] Faculty of Geology, University of Warsaw, Żwirki i Wigury 93, 02-089 Warszawa, Poland
[d] Faculty of Mining and Geology, University of Belgrade, Djusina 7, 11000 Belgrade, Serbia
[e] Kazan Federal University, Kremlovskaya 18, 420008 Kazan, Russia
[f] Department of Biochemistry and Environmental Chemistry, The John Paul II Catholic, University of Lublin, Konstantynów 1 I, 20-708 Lublin, Poland

HIGHLIGHTS

- The GWP of the gases released by xylitic lignite was the lowest among the samples.
- Extraction of the detritic lignite may reduce GHG emissions from the abandoned mines.
- Detritic lignites show the potential to serve as a source of coalbed methane.

GRAPHICAL ABSTRACT
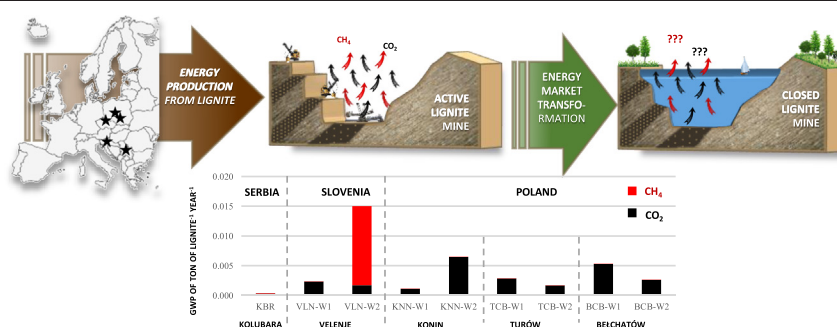
ABSTRACT

Due to changes in the energy market, it is projected that lignite excavation will be reduced in the near future. Cessation of exploitation is associated with restitution of natural water conditions and flooding of the resources left in the mines. Flooded lignite mines are a potential source of greenhouse gases (GHG) (CH_4, CO_2 and N_2O), which should be monitored due to growing environmental concerns. Here, we aim to recognize GHG release from the lignites collected from the main deposits of Poland, Slovenia and Serbia. GHG production was studied along with a range of physical and chemical parameters that are crucial for microbial growth and activity.

The microcosm experiments showed that the main gas emitted from the lignites was carbon dioxide. Daily CO_2 production was highly variable. The highest values were recorded for detroxylitic lignite collected from the Konin deposit (402.05 nmol CO_2 g^{-1} day^{-1}) while the lowest were for the Kolubara xylitic lignite (19.64 nmol CO_2 g^{-1} day^{-1}). Methane production was much lower and ranged from nearly zero to 66.75 nmol g dry mass^{-1} d^{-1}. Nitrous oxide production was not detected. It was found that CO_2 production, being a general measure of microbial activity, was positively affected by NO_3^- concentration and redox potential. With respect to methane formation, the lower atmospheric oxygen exposure of the sample from the Velenje underground mine compared to the samples from the opencast mines has been identified as a possible cause of the high methane production. The overall global warming potential (GWP) of the gases released by xylitic lignite was lowest among the samples. Preferential extraction of the detritic lignites is suggested as a means to reduce GHG emissions from the abandoned lignite mines.

* Corresponding author at: Department of Natural Environment Biogeochemistry, Institute of Agrophysics, Polish Academy of Sciences, Doświadczalna 4, 20-290 Lublin, Poland.
E-mail address: apytlak@ipan.lublin.pl (A. Pytlak).

1. Introduction

Lignite (brown coal) deposits are located all over the world. Seams of this raw material are usually located at shallow depths, allowing for opencast mining. The relatively easy accessibility and the lower level of natural hazard in comparison to the exploitation of hard coal has made lignite an important source of energy. In 2019, 27 countries declared using this resource. In many of them, the combustion of lignite contributed to the generation of a significant part of the energy produced (e.g., Poland 33-35%; Nyga-Lukaszewska et al., 2020). Importantly, nearly half of all lignite is mined and utilized in Europe (Knoema, 2020).

The extraction and combustion of coal pollutes water, soil, and especially the atmosphere. Air pollution generated by the mining industry has both a local (particulate matter, sulphur and nitrogen oxides) and a global impact (greenhouse gases, GHG). GHG emissions are of particular concern because coal mining and burning comprise a high proportion of the anthropogenic sources of both CH_4 and CO_2 (Saunois et al., 2020). The intensification of climate change and the degradation of the natural environment in many areas of the world has instigated the currently global trend to replace coal with renewable energy sources that are more friendly to the environment and human health (EIA, 2020; IEA, 2020).

Due to the changes taking place in the energy market, it is projected that in the short-to-medium term, most lignite-fired power plants will be closed, making lignite excavation unnecessary (Alves Dias et al., 2018). It is expected that this will reduce the scale of anthropogenic GHG emissions, as the coal will no longer be transported and burned. However, as recently described by Kholod et al. (2020), a substantial proportion of GHG emissions come directly from disrupted geological formations and this will continue for decades, regardless of the cessation of industrial exploitation of the seams. Particularly, the extent of GHG emissions from unexploited (and abandoned) lignite remains largely unrecognized. Both the guidelines for national greenhouse gas inventories (Eggleston et al., 2006) and the recently updated version indicate that "surface mines may continue to emit methane as the gas leaks from the coal seams that were broken or damaged during mining" but "there are at present no methods for estimating emissions from this source" (Buendia et al., 2019). Therefore, there is an important gap in the knowledge that needs to be addressed.

The available projections for GHG emissions from closed mines mainly concern underground exploitation. The estimates are based on the current methane bearing capacity and apply Langmuir equations to quantify gas desorption (e.g., Kholod et al., 2020). In the case of hard coals, which are resistant to biodegradation, these calculations are justified. However, bioavailability of the organic matter for microbial processes increases with decreasing thermal maturity (Robbins et al., 2016) and in the case of brown coal, particularly lignite, it seems reasonable to also take into account biological de novo formation of GHG.

The coal seams were shaped by an anaerobic environment in which it was possible to conserve the deposited organic matter. In the course of exploitation, lignite deposits are drained and exposed to atmospheric conditions. Such a drastic change in the living conditions of the microbiota alters the rate, extent and direction of biological processes. However, with the end of mining operations and cessation of drainage works, most mine workings will naturally be flooded with water. This may lead to the restoration of anaerobic conditions in the deposit and the reactivation of processes the lead to the formation of potent GHG, i.e., CH_4, CO_2 and N_2O. Here, we hypothesize that GHG formation occurs in abandoned and submerged lignites. We also aim to recognize the GHG production potential of lignites collected from the main lignite deposits exploited in Poland, Slovenia and Serbia, which represent various lithotypes, ages and burial histories. GHG production was studied along with a range of physical and chemical parameters that are crucial for microbial growth and activity.

2. Materials and methods

2.1. Sampling sites

Lignites were collected from 5 active coal mines located in Central Europe. In Poland, these were the Bełchatów, Turów and Konin opencast mines, which together are responsible for ca. 95% of the country's lignite production (Polish Geological Institute, 2020). In Serbia, sampling was performed in the Kolubara opencast mine which supplies nearly 75% of the country's lignite (Public Enterprize Electric Power Industry of Serbia, 2020). In Slovenia, samples were obtained from the country's only working coal mine Velenje; a mine which uniquely employs the underground exploitation method.

2.2. Geological settings of the sampled deposits

2.2.1. Poland

The majority of Poland's territory belongs to the European Paleogene–Neogene Basin. The lignite-bearing areas cover approximately 70,000 km^2, which is about one-third of the Poland's territory. Lignite deposits mainly occur in the western, southern and central parts of the country and were formed in epeirogenic depressions from the Palaeocene up to the Upper Miocene (Fig. 1). Polish lignites represent humic low rank coal. Industrial exploitation is performed mainly in the Lower and Middle Miocene formations i.e., the third Ścinawa lignite seam (ŚLS-3), the second Lusatian lignite seam (LLS-2), and the first Mid-Polish lignite seam (MPLS-1) (Kasinski et al., 2010; Mastej et al., 2015; Widera, 2016a, 2012).

2.2.2. Konin (KNN)

The mine exploits Mid Miocene lignites located to the north of the city of Konin (52°45′57′′N, 18°53′26′′E) and were deposited in a shallow tectonic depression with a Mesozoic basement. Lignite formations are associated with MPLS-1 (Widera, 2016b). The seam thickness is 3-20 m and is overlain by grey, clayey quartz sands of the Adamów Formation (Kasinski et al., 2010; Piwocki, 1992). The basement of the lignite deposit is represented by marly and sandy limestones (Ciuk, 1991). The lithostratigraphic unit of the Konin coal mine is characteristic of mires, wet forests and fen or shallow water (Widera, 2016b).

2.2.3. Bełchatów (BCB)

The Bełchatów coal basin (central Poland, 51°15′46″N 19°18′49″E) is located in the Alpine orogeny-aged Kleszczów Graben. The deposit consists of two lignite fields separated by the Dębina Salt Dome containing Upper Permian (Zechstein) evaporites. Palaeogene and Neogene filling of the graben is underlain by Upper Jurassic limestones and Upper Cretaceous gaizes. The productive coal complex is considered to be an equivalent of ŚLS-3 (in the lower part) and LLS-2 (in the upper part) (Pawelec and Bielowicz, 2016; Widera, 2016b).

2.2.4. Turów (TCB)

The Turów coal deposit is located in the Zittau Basin (on the border of Germany, Poland and the Czech Republic) (50°91′24′′N 14°90′31′′E). It fills a Tertiary tectonic depression which was formed in the northwestern part of the Ohre rift system. The TCB is filled with a Miocene brown-coal formation and clastic Cenozoic deposits underlain by igneous rocks. The lignite seams documented in the TCB are of a similar age to those found in the BCB (ŚLS-3 and LLS-2). However, unlike other Polish lignites, they were affected by tectonic and volcanic activity (Liber-Makowska, 2013).

2.2.5. Serbia – Kolubara

Reserves of the Kolubara coal basin are located in the central region of Serbia (44°47′15′′, 20°22′49′′). The Upper Miocene sediments were formed in the Pannonian Basin System in shallow lacustrine, delta plain and fluvial environments. The freshwater coal-bearing series of
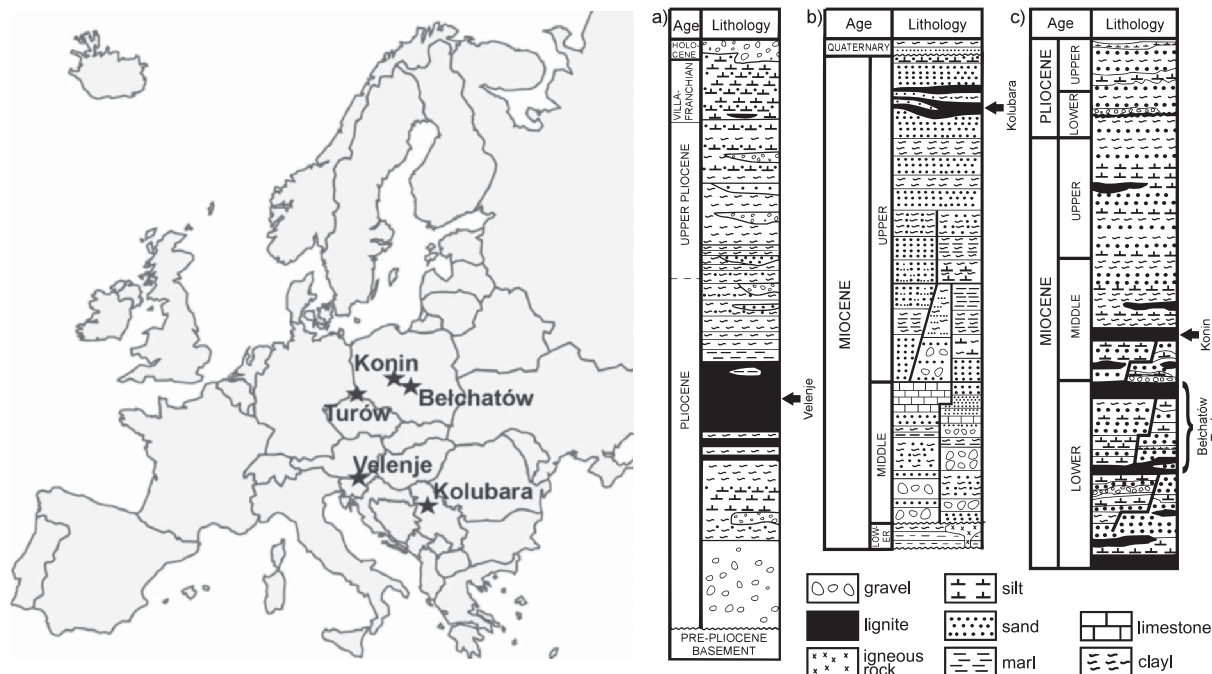
Fig. 1. Location and schematic lithostratigraphic profiles of the studied lignite deposits in Slovenia (a), Serbia (b) and Poland (c). Position of lignite seams is indicated by arrows (modified from (Fabianska, 2007; Kanduc and Pezdic, 2005; Životic et al., 2013).

the Kolubara Basin consist of sand, clay and three coal seams: seam III - Lower coal seam, seam, II - Main coal seam, and seam I -Upper coal seam (Kezovic, 2011). Coal from the Kolubara Basin is typical lignite with a high moisture content, lower net calorific value and a huminite reflectance of 0.30 ± 0.03 (Životic et al., 2013).

2.2.6. Slovenia - Velenje

The Velenje coal mine is located in the central region of the Velenje Basin in NE Slovenia (46°37′21′′, 15°06′68′′). The Velenje Basin is a mountainous pull-apart basin, bounded by the Smrekovec and Sostanj faults, which belong to the Periadriatic fault. Tectonic activity created an accommodation space filled with Pliocene and Quaternary sediments up to 1000 m in thickness (Brezigar, 1985). Velenje lignite was formed in a marsh environment (Brezigar et al., 1985). The main lignite seam is characterized by a thickness of up to 165 m in the central part of the seam with an average of 60 m (Liu et al., 2019).

2.3. Sampling procedures

Lignite was sampled from freshly exposed fragments of each deposit. Large lignite chunks (4 - 5 kg) were immediately put into hermetic containers and tightly closed. Lithotypes were distinguished on the basis of two lithotype components i.e., xylites and detritus using the "10% rule" (International Committee for Coal Petrology, 1993; Widera, 2012). Prior to laboratory analysis (chemical, physical and incubation experiment), lignite subsamples were aseptically crushed to $\varphi < 2$ mm in anaerobic conditions in a glove box (Labconco, USA, atmosphere of nitrogen).

2.4. Physical and chemical analysis

The moisture of the lignites was determined gravimetrically by oven-drying to a constant weight at 105 °C. Reaction (pH), oxidation-reduction potential (Eh) and electrolytic conductivity (EC) were determined using a multifunctional potentiometer pIONneer 65 (Radiometer Analytical S.A., France) equipped with a glass electrode (Cartrode pH E16M340), combined platinum and Ag/AgCl (E31M004) electrode and

EC conductivity cell (CDC 30 T-3), respectively. Carbon content (total organic – TOC and total inorganic – IC) was determined by dry combustion using a TOC-VCSH with SSM-5000A module (Shimadzu, Japan). A detailed description of these analytical methods can be found at Szafranek-Nakonieczna et al. (2018). The availability of biogenic compounds (N-NO$_3$, N-NH$_4$ and P-PO$_4$) was analysed according to detailed protocols as presented previously by Stepniewska et al. (2013).

2.5. Microcosm experiment

Analogously to the previously described experiments (Pytlak et al., 2020b, 2020a; Szafranek-Nakonieczna et al., 2018), microcosms with the aim of determining the biological formation of CH_4 and CO_2 were prepared in a glove box, under N_2. Ten grams of aseptically crushed lignite was placed in dark glass bottles (total capacity 60 cm^3) and supplemented with an appropriate volume of a deionised water to achieve 200% of total water capacity (reflect natural conditions). The bottles were tightly closed with a rubber septa and aluminium cap to allow for headspace gas sampling. Measurements were conducted at 30 °C. Triplicate samples were prepared for each treatment.

The concentrations of gases (CH_4, CO_2) during the experiment were determined using a Varian 3800 gas chromatograph equipped with flame ionization (FID, 200 °C) and thermal conductivity (TCD, 120 °C) detectors. Gases were detected after separation of the sample on a CP-PoraPLOT Q 25 m × 0.53 mm ID, 20 μm film and a Molecular Sieve 5A 30 m × 0.53 mm ID columns connected together. Injector temperature was set to 120 °C and oven temperature was set to 40 °C. Helium was used as the carrier gas.

Methane and carbon dioxide production rate was determined based on the linear increase in the concentration of a given gas in time and expressed as a nmol per gram dry mass per day (nmol g^{-1} day^{-1}).

2.6. Global warming potential (GWP) calculations

The GWP for each lignite was calculated for the 100 year horizon, including climate-carbon feedback as an CO_2 equivalent by multiplying

average daily CH_4 emissions by the conversion factor of 34 (Myhre et al., 2013).

2.7. Statistical methods

The Spearman rank-order correlation coefficient was used to measure the strength and direction of association between GHG release rate and environmental parameters. Calculations were performed using Statistica 13 (TIBCO Software Inc.). A graphical display of the correlation matrix was created using the "Heatmap illustrator" package in TBtools (Chen et al., 2020). $p < 0.05$ was considered statistically significant. Bray-Curtis similarity matrices representing the studied physical and chemical properties were analysed using non-metric multidimensional scaling (NMDS) in PAST 4.03 (Hammer et al., 2001). NMDS was used to detect patterns that could explain the observed similarities and dissimilarities among the samples.

3. Results and discussion

3.1. Physical and chemical properties

The lignites used here are characterized by various lithotype, age and location (Table 1). They did show some similarities, e.g., TOC content (55–68% range). Only PGB-W1 contained more mineral matter, which resulted in a reduced TOC (39%) (Table 2). Generally, the TOC content of the studied materials corresponded with their rank (Strapoc et al., 2011). The reaction of the analysed lignites was also alike and in the neutral range (pH 6–7.7). The exception was KNN-W2, which was acidic (pH 3.45) (Table 3). With regard to the remaining parameters, e.g., concentrations of biogenic N and P, or overall EC, a large range of observed values was found, even in samples extracted from the same deposit (Table 2, Table 3). An example of this is the availability of P-PO_4 in the Bełchatów samples, which ranged from 0.58 mg kg^{-1} (PGB—W1) to as much as 19.4 mg kg^{-1} (PGB—W2). These differences indicate that there is a variation in the living conditions of the microorganisms present in lignite, which may be reflected in the ability of the microbiota to produce greenhouse gases.

However, the parameter that predominantly determines the production of GHG is the oxidation-reduction potential (Eh) (Wang et al., 1993; Yu et al., 2006). Eh measures the abundance of oxidized and reduced chemical substances and enables the prediction of what electron acceptors are available for biogeochemical processes (Fiedler et al., 2007). Redox potential is tightly related with the activity of microbial communities (Fig. 2) and in general, Eh values are positively correlated with CO_2 production, while its relationship with CH_4 production is the reverse (Chabbi et al., 2006; Wang et al., 1993).

The redox potential of the studied samples ranged between 282 and 395 mV (Table 3), which places the lignites in the range characteristic for suboxic or moderately reduced environments (Fiedler et al., 2007). The only distinctive sample was KNN-W2 whose Eh was as high as 720 mV, meaning that at the beginning of the experiment, the availability of electron acceptors in this lignite was comparable to oxic, well aerated soil. As a rule, pH and Eh values are negatively correlated (Fiedler

et al., 2007). The interdependence of these parameters as determined in the studied lignites is consistent with this rule (Fig. 3) and KNN-W2, the most acidic sample, was also characterized by the highest Eh values (Table 3). However, even after correction to Eh_7 (using $Eh_7 = Eh$ (mV) + 59 (mV) (pH - 7.0) adapted from Martin et al. (2013)), the Eh value for KNN-W2 (510 mV) still lies in the range characteristic for oxic conditions (Fig. 2). Bearing in mind that samples were collected immediately after excavation and kept hermetically closed, the KNN-W2 lignite must have been exposed to in situ oxidative conditions prior to excavation. This may be possible, due to the fact that the Konin deposit is built of a number of scattered, relatively small (in comparison to other deposits studied) lignite seams, and covered by thin overburden (Meissner, 1962). Exploitation of the adjacent fields, in particular their dewatering, could lead to the groundwater table lowering and air intrusion into the coal-bearing strata, even prior to overburden removal from the KNN-W2 sampling area. The low pH itself also indicates the occurrence of aerobic processes. Lignite-bearing strata, including the one in the Konin area (Gilewska and Otremba, 2015), contain pyrite. When pyrite is exposed to air, in the presence of humidity, it is oxidized, forming sulphuric acid (Dos Santos et al., 2016). This process contributes to the acidification of the environment and may increase the pore solute concentration. This is because, unlike pyrite, sulphuric acid is water-soluble. Indeed, the EC values measured in the samples collected from the Konin deposit were high, especially in KNN-W2 (Tables 3, 1.42 mS cm^{-1}).

Eh was also tightly related to speciation of the available nitrogen (Fig. 3). The Spearman's rank correlation values for Eh and N-NO_3 were 0.49 ($p < 0.05$), while for N-NH_4 0.52 ($p < 0.05$), suggesting that the more reduced lignites contained higher concentrations of the reduced N form. Because N-NH_4 was the dominant form of nitrogen (with concentrations several dozen times higher than those of N-NO_3), it may be assumed that, generally, the lower Eh promoted N_2 availability. This is important because nitrogen is one of the major factors controlling microbial growth rate.

It seems that the oxidative conditions that occurred in KNN-W2 could also lead to the partial decomposition of the lignite. TOC of this sample (55.96%) was significantly lower than in the other sample collected from the same basin (KNN-W1, 65.65% TOC, Table 3).

The NMDS ordination plot, based on the physical and chemical properties of lignites, shows that there was significant separation among the samples (Fig. 4). This confirms that the studied materials created distinct environmental niches and points to the fact that the indigenous microbial communities inhabiting the lignites may carry out different biogeochemical processes. Environmental vector fitting shows the associations between geochemical parameters and the NMDS axes. The most important were Eh, TOC and N-NO_3, which were strongly correlated with both NMDS axes. These parameters governed the distribution of the majority of points, which were clustered together along Eh-NO_3 vector. Points representing samples characterized by the highest Eh and N-NO_3 values (KNN-W2) formed a separate group. One of the apparently dissimilar points were those denoting lignite from the Kolubara mine (KBR). The distinctiveness of this lignite may result from the fact that KBR was the only exclusively xylitic lignite, which contained a very low amount of soluble compounds (manifested low

Table 1
Lithostratigraphic characteristics of the sampled lignite beds.

Symbol	Location	SEAM	Age	Lithotype
KBR	Kolubara	Main seam	Upper Miocene	Xylitic
VLN-W1	Velenje	Main seam	Pliocene	Xylodetritic
VLN-W2	Velenje	Main seam	Pliocene	Detritic
KNN-W1	Konin	First Mid-Polish lignite seam	Middle Miocene	Detritic
KNN-W2	Konin	First Mid-Polish lignite seam	Middle Miocene	Detroxylitic
PGT - W1	Turów	Third Ścinawa lignite seam	Lower Miocene	Detroxylitic
PGT - W2	Turów	Second Lusatian lignite seam	Lower Miocene	Detroxylitic
PGB - W1	Bełchatów	Second Lusatian lignite seam	Lower Miocene	Detroxylitic
PGB - W2	Bełchatów	Third Ścinawa lignite seam	Lower Miocene	Detritic

Table 2
Characteristics of the investigated coals and lignites. TOC – total organic carbon; N-NO3, N-NH4P-PO4, SD – standard deviation (sample abbreviations as in Table 1).

Symbol	Moisture		TOC		N-NO3		N-NH4		P-PO4	
	%		%		mg kg dry mass^{-1}					
	Mean	±SD	Mean	±SD	Mean	±SD	Mean	±SD	Mean	±SD
KBR	51.92	1.31	63.26	1.88	0.11	0.02	37.57	0.51	6.55	0.74
VLN-W1	23.58	0.37	66.73	2.62	0.00	0.00	94.86	0.93	7.03	1.56
VLN-W2	24.22	0.56	65.41	5.50	0.00	0.00	48.60	0.70	5.44	2.89
KNN-W1	49.71	0.58	65.65	2.63	0.00	0.00	15.77	1.18	1.57	0.20
KNN-W2	43.97	1.26	55.96	2.99	2.26	0.01	24.42	0.46	9.78	0.76
PGT - W1	80.99	3.11	67.31	2.12	0.94	0.86	27.54	11.55	2.64	1.19
PGT - W2	66.57	6.50	68.38	3.09	0.41	0.13	25.13	6.24	9.39	6.33
PGB - W1	69.74	13.31	39.05	2.18	4.68	0.87	28.94	12.35	0.58	0.73
PGB - W2	62.39	4.58	65.29	2.52	1.54	1.98	38.46	3.33	19.41	12.77

EC values). Outlying points were additionally those representing VLN-W2 i.e., the detritic lignite from the Velenje lignite mine. Further statistical analysis, performed with the use of ANOSIM, confirmed that there were significant differences between the lignites. The most important variable determining similarity/dissimilarity of the lignites in terms of physico-chemical properties was age ($R = 0.72$, $p < 0.01$). Lithology appeared to be less important. ANOSIM R values of 0.34 show that the generally properties of lignites, representing various lithologies, overlap. Pairwise comparisons revealed that the most dissimilar was the xylitic lignite, which remains consistent with the NMDS orientation (Fig. 4).

3.2. GHG release

The microcosm experiments showed that the main gas released from the lignites was carbon dioxide. Daily CO_2 production was several hundred times higher than that of CH_4. KNN-W2 and BCB-W1 lignites released particularly high amounts of CO_2, reaching 402.05 and 328.63 nmol CO_2 g^{-1} day^{-1}, respectively. The smallest activity was found in the Kolubara lignite, which released only 19.64 nmol CO_2 g^{-1} day^{-1} (Fig. 5a).

Desorption of CO_2 gas from lignites requires the consideration of both physical desorption and biological de novo formation, which co-occur. It is a well-known phenomenon that low rank coals adsorb CO_2 and that (due to competition for active sites between water and CO_2 molecules) the sorption capacity decreases with increased moisture (Liu et al., 2016). It was suggested that detroxylytic and xylodetritic lignites have a higher CO_2-binding capacity than xylitic ones (Bielowicz and Baran, 2019). The reason may be that the xylite-rich materials have massive structure (Widera, 2016b) with remarkably lower porosity (Bielowicz and Baran, 2019) thus providing fewer available biding sites for CO_2. In fact, within the studied samples, xylitic lignite from Kolubara released the smallest amount of CO_2 (Fig. 5a.).

It has also been suggested, that among lignites, CO_2 sorption capacity increases with the degree of coalification (Bielowicz and Baran, 2019). This relationship, however, was not noted in the results presented here. Among the studied samples, the most mature were lignites from the Turów mine. Organic matter accumulated in this coal basin is

subjected to considerable geothermal heating (Liber-Makowska, 2013) which results e.g., in higher (in comparison to other Polish lignites) cyclization of aromatic rings (as evidenced by FTIR) (Pytlak et al., 2020a). Yet, in spite of the apparent differences in maturity, CO_2 emissions from Turów lignites were close to the average calculated for the studied set of materials. This shows that the observed variability in CO_2 emissions cannot be fully explained by physical sorption.

The fact that lignites are a habitat for a vast array of microorganisms has already been described in detail (e.g., Bucha et al., 2018; Detman et al., 2018; Pytlak et al., 2020a; Strapoc et al., 2011). A separate and debatable issue remains as to whether all of the marked taxa actually realize their ecological niche in the lignite. This is because conditions that occur in the deposit do not often stay in line with the known ecophysiology of the bacterial taxa (Pytlak et al., 2020a). Nevertheless, the activity of microbial communities can be assessed via respiration, it being a universal measure of microbial vital processes (Haney et al., 2018).

Further evidence for biological CO_2 production in the lignites it is reflected by the positive relationship with Eh values (Spearmann 0.46, $p < 0.05$). This interdependence persists because the electron acceptors
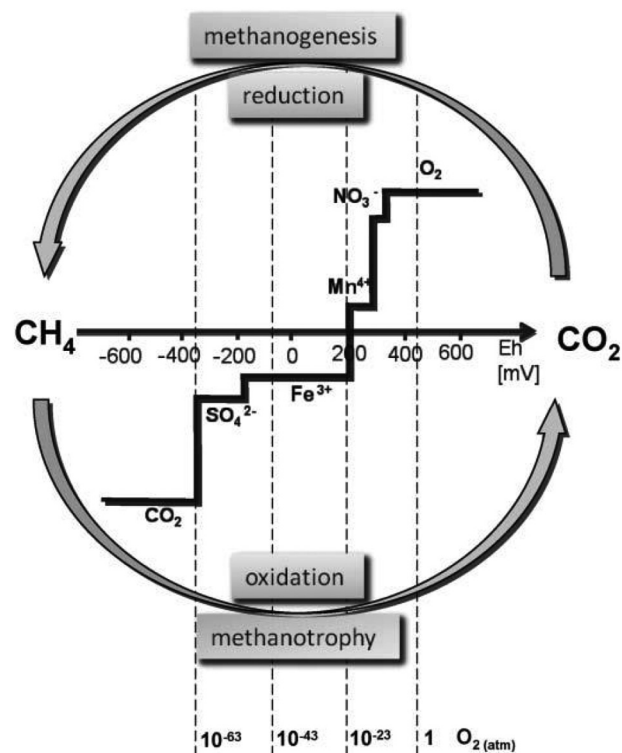
Table 3
pH, Eh and EC of the studied lignites (sample abbreviations as in Table 1).

Symbol	pH		Eh (mV)		EC (mS cm^{-1})	
	Mean	±SD	Mean	±SD	Mean	±SD
KBR	6.44	0.05	282	1.2	0.14	0.01
VLN-W1	7.28	0.05	296	7.6	0.31	0.00
VLN-W2	7.57	0.11	311	1.0	0.90	0.02
KNN-W1	6.02	0.05	383	4.7	1.03	0.00
KNN-W2	3.45	0.23	720	9.7	1.42	0.01
PGT - W1	7.71	0.03	346	0.1	0.58	0.00
PGT - W2	6.25	0.03	369	4.5	0.57	0.00
PGB - W1	6.83	0.01	370	0.3	0.33	0.00
PGB - W2	5.94	0.00	395	1.6	0.91	0.00

Fig. 2. Redox potential range showing microbial carbon metabolism and electron acceptors (modified from Pytlak et al., 2014; Schlesinger, 1997).
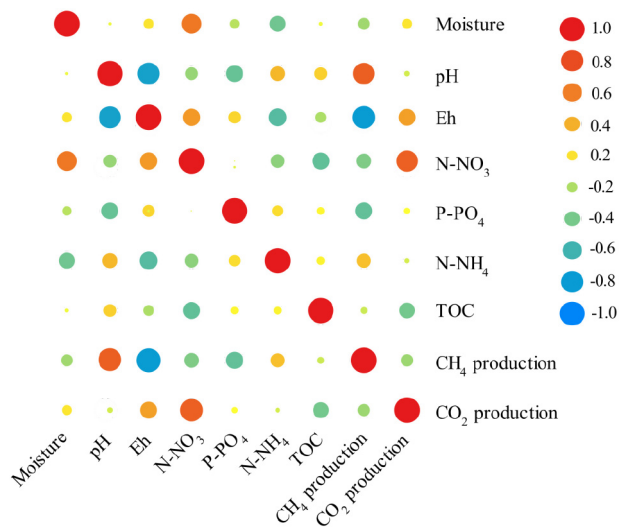
Fig. 3. Correlogram of Spearman's rank correlation coefficients of the physical and chemical properties as well as greenhouse gases (GHG): CO_2 and CH_4 production by the lignites (based on data presented in Tables 2, 3 and Fig. 5).

available at higher Eh enable higher free Gibbs energy to be released during oxidation-reduction reactions. The amount of available energy is reflected in the intensity of the microbial catabolic processes (Lian et al., 2016). In addition, after O_2, NO_3^- is the second most potent electron acceptor and it explains the positive relationship between CO_2 release and NO_3^- concentration (Fig. 3). The relevance of CO_2 emission and Eh interdependence has already been described from other environments, such as soil and sediment (e.g., Chabbi et al., 2006; Wang et al., 1993). The occurrence of this dependency also in the current dataset confirms that microbially-driven biogeochemical processes take place in these anthropogenically affected lignite-bearing sedimentary basins and that their intensity is redox-related.

Previous studies concerning the microbial degradation of low-rank coals state that detritic lignite is more susceptible to decomposition than xylitic (Hofrichter and Fakoussa, 2001), which consists mainly of solid, fossilized wood fragments such as trunks, branches and roots (Widera, 2012). Lignin (and lignin-derived macerals), being the main component, is considered the most difficult portion of plant biomass to degrade (DeAngelis et al., 2011). It has also been suggested that fossilized resin, fixed in the form of terpenoid compounds, acts as an antimicrobial agent (Bechtel et al., 2007; Otto and Simoneit, 2001).

Therefore, the low CO_2 emissions from the KBR xylitic lignite can also be explained biologically (Fig. 5a).

Methane release was highly variable among the investigated lignites and ranged from ~0 to 66.75 nmol g dry mass^{-1} d^{-1} (Fig. 5b). It should be noted that among the analysed mines, Velenje is the only one carrying out underground exploitation and therefore the high methane formation in the VLN-W2 lignite may be due to the lower exposure to oxygen conditions compared to those experienced by the lignites of the opencast mines. This hypothesis seems to be confirmed by a strong, negative dependence between Eh values and CH_4 production (Spearman -0.8, p < 0.05) (Fig. 3). The low tolerance of methanogens to aerobic conditions is due to the fact that their metabolic pathways are based on extremely oxygen-sensitive enzymes (e.g., containing Fe—S cluster) (Sheehan et al., 2015; Sikora et al., 2017). Their deactivation leads to the loss of energy conservation by microbiota and as a consequence cessation of methane production.

Interestingly, xylodetritic lignite extracted from the same mine was more than 600 times less effective in methane formation. This disparity seems to be related to the low susceptibility of xylitic lignites to biological degradation. Methanogens are capable of utilizing only a narrow range of substrates such as H_2/CO_2, formate, acetate, methanol, and methylated compounds. Methanogenesis is in fact a multistage process in which exact CH_4 formation by methanogenic *Archaea* is preceded by the degradation of complex organic molecules by a consortium of various microorganisms, mostly bacteria. Degradation of the lignin-derived xylites could therefore constitute a bottleneck in methanogenesis, as is the case in other environments (Cater et al., 2014). The results consistent with this theory, indicating greater production of methane from detritic lignites, can also be found in the work of Bucha et al. (2020), who compared the biotechnological potential (in the context of biogas production) of lignites with different lithology. It is also suspected that some of the lignin degradation intermediates (phenyl acids) hinder anaerobic mineralization of organic materials (Prem et al., 2021).

3.3. Nitrous oxide formation

Nitrous oxide is approximately 265 times more potent than CO_2 in atmospheric warming and contributes to stratospheric ozone depletion (Liu et al., 2020). Most anthropogenic emissions of this gas occur in drained peatlands (Liu et al., 2020). Peat and lignite have a similar genesis and, despite differences resulting from age, many features in common (Höök, 2012; Widera et al., 2007). Therefore, it is supposed that lignites could also be a source of GHG. However, N_2O was not detected in any of the studied microcosms. The explanation of this phenomenon is, first of all, the speciation of N_2, which in the lignites was available
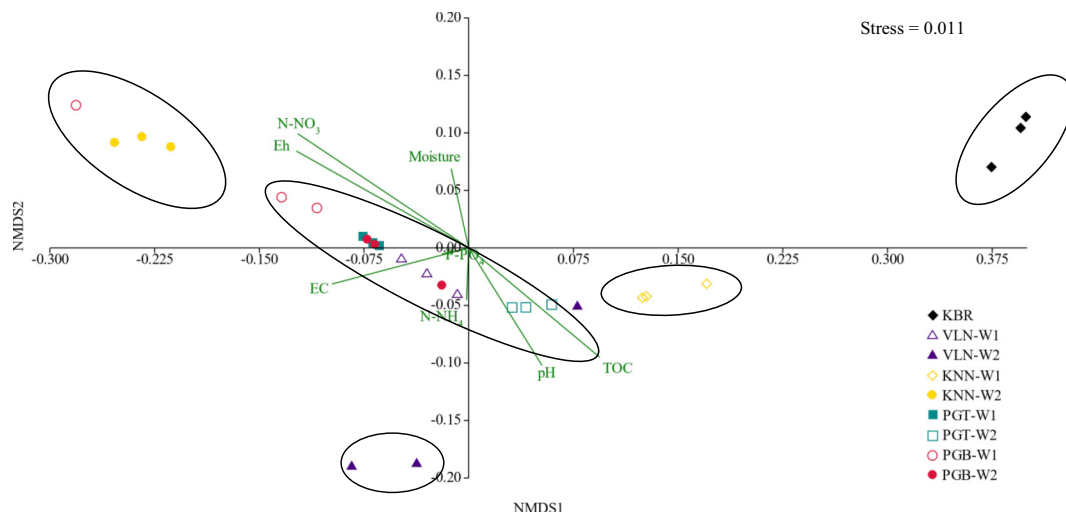

Fig. 4. Nonmetric multidimensional scaling (NMDS) plot based on the Bray-Curtis distances of lignite properties (based on data from Tables 2 and 3, sample abbreviations as in Table 1.).
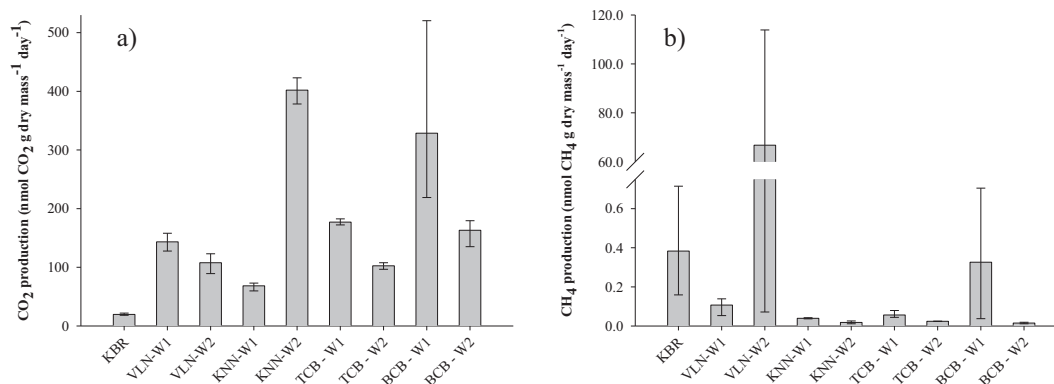
Fig. 5. Greenhouse gases (GHG) production rate of CO_2 (a) and CH_4 (b) in the studied lignites. Mean values $\pm$ SD. Sample abbreviations as in Table 1.

mainly in reduced form. N_2O is produced either by nitrification in the presence of O_2 or by denitrification in anoxic conditions (Khalil et al., 2004; Liu et al., 2020). The transition of NH_4 to N_2O by nitrification requires the availability of oxygen, the concentration of which is a factor that significantly determines the rate of the process (Khalil et al., 2004). The experimental treatments were oxygen-free so nitrification could not occur. On the other hand, availability of NO_3^-, which could be a source for anaerobic N_2O formation via denitrification, was scarce. The observed effect seems to be consistent with the results presented by Liu et al. (2020) who pointed out that rewetting of the peatlands effectively reduces N_2O emissions.

3.4. Environmental impact of flooded lignites

Results concerning GHG production by flooded lignites suggest that they would mainly release CO_2. Methane emissions were significantly lower and even given the GWP of methane (which is several dozen times higher than CO_2), CO_2 played a dominant role (Fig. 6).

That lake ecosystems are able to buffer GHG emissions depends on many local factors. In the case of CO_2, it is perfectly soluble in water but this leads to acidification of the water (Cole and Prairie, 2014). Post-mining waters are also threatened by acidification caused by the oxidation of sulphides (Gläßer et al., 2011). At low pH, the water solubility of CO_2 decreases substantially, thus, water chemistry has a huge impact on the buffering of lignite-originating CO_2 emissions. Lake ecosystems are also a habitat of methanotrophic bacteria, which may effectively reduce methane emissions. However, the majority of mesophilic methanotrophic bacteria prefer close to neutral pH (Islam et al., 2020), hence local geology (affecting pH buffering capacity of water) plays an important role in the regulation of GHG emissions from flooded lignites.
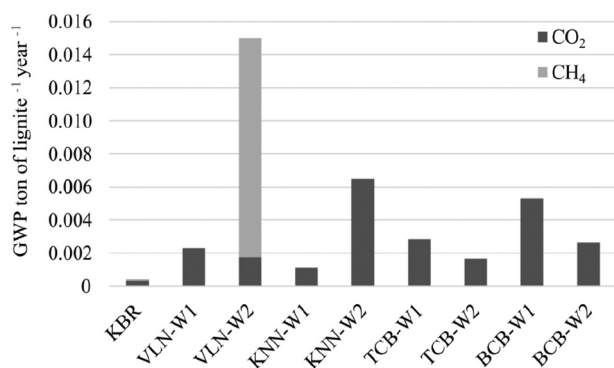

Fig. 6. Global warming potential (GWP) of the studied lignites. GWP for CH_4 was calculated for the 100 year horizon, including climate-carbon feedback with a conversion factor of 34 (Myhre et al., 2013). Sample abbreviations as in Table 1.

It should be remembered that methanotrophic bacteria are also a natural component of the microbiome of coal, lignites and the surrounding geological formations (Pytlak et al., 2021, 2020a, 2014; Stepniewska et al., 2014, 2013; Stepniewska and Pytlak, 2008). These microorganisms prefer microoxic conditions. It has been shown that in high humidity conditions they are able to utilize methane with high efficiency. Therefore, they can potentially contribute to limiting the stream of methane emitted to the atmosphere from unexploited parts of the abandoned deposits. Nevertheless, as in the case of microorganisms occurring in the water column, the activity of methanotrophs present in lignites depends on the physicochemical changes in the environment.

4. Conclusions

The obtained results show that the size and nature of the GHG emissions depend on the lithotype of brown coal. The lowest impact on the environment was found in xylitic lignite (with GWP of 3.91×10^{-4} per ton annually), while the lignites containing the detritus component released significantly more GHG (with GWP up to 1.5×10^{-2} per ton annually). These results may be an indication of how to plan coal seam exploitation. Our suggestion is that preferential extraction of detritic coals from opencast mines may reduce future GHG emissions. On the other hand, the detritic lignites that are exploited via the underground method (Velenje mine) show the potential to serve as a source of coalbed methane to be captured and utilized for energy-generation purposes. The development of precise models enabling the prediction of GHG emissions from lignites still require the analysis of a larger number of samples, but our data confirm that flooded lignites may substantially contribute to GHG emission. Furthermore, lithology and time of exposure to oxygen conditions should be taken into account as they have a significant impact on the shape of the microhabitat and direction of organic matter transformation that occurs in the unexploited part of the deposit.

CRediT authorship contribution statement

Anna Pytlak: Conceptualization, Investigation, Formal analysis, Writing, Methodology, Visualization; Anna Szafranek-Nakonieczna: Investigation; Weronika Goraj: Investigation; Izabela Śnieżyńska: Writing, Visualization; Aleksandra Krążała: Writing; Artur Banach: Investigation; Ivica Ristović: Resources; Mirosław Słowakiewicz: Resources; Zofia Stępniewska: Resources, Funding acquisition.

Funding

Declaration of competing interest

The authors declare that they have no known competing financial interests or personal relationships that could have appeared to influence the work reported in this paper.

References

Alves Dias, P., Kanellopoulos, K., Medarac, H., Kapetaki, Z., Miranda-Barbosa, E., Shortall, R., Czako, V., Telsnig, T., Vazquez-Hernandez, C., Arántegui, L.R., Nijs, W., Aparicio, G., Trombetti, M., Mandras, G., Peteves, E., Tzimas, E., 2018. EU Coal Regions: Opportunities and Challenges Ahead (JRC112593 EUR 29292 EN) Luxembourg.

Bechtel, A., Widera, M., Sachsenhofer, R.F., Gratzer, R., Lücke, A., Woszczyk, M., 2007. Biomarker and stable carbon isotope systematics of fossil wood from the second lusatian lignite seam of the Lubstów deposit (Poland). Org. Geochem. 38, 1850–1864. https://doi.org/10.1016/j.orggeochem.2007.06.018.

Bielowicz, B., Baran, P., 2019. CO2 sorption properties of selected lithotypes of lignite from polish deposits. Geol. Q. 63, 786–800. https://doi.org/10.7306/gq.1508.

Brezigar, A., 1985. Premogova Plast rudnika lignita Velenje. coal seam of the Velenje coal mine. Geologija 28 (29), 319–336.

Brezigar, A., Kosi, G., Vrhovsek, D., Velkovrh, F., 1985. Paleontoloske raziskave pliokvartarne skladovnice velenjske udofine. paleontological investigations of the plio-quaternary beds of the Velenje depression. Geologija 28 (29), 93–119.

Bucha, M., Jedrysek, M.O., Kufka, D., Plesniak, L., Marynowski, L., Kubiak, K., Blaszczyk, M., 2018. Methanogenic fermentation of lignite with carbon-bearing additives, inferred from stable carbon and hydrogen isotopes. Int. J. Coal Geol. 186, 65–79. https://doi.org/10.1016/j.coal.2017.11.020.

Bucha, M., Detman, A., Plesniak, L., Drzewicki, W., Kufka, D., Chojnacka, A., Mielecki, D., Krajniak, J., Jedrysek, M.O., Sikora, A., Marynowski, L., 2020. Microbial methane formation from different lithotypes of miocene lignites from the Konin Basin, Poland: geochemistry of the gases and composition of the microbial communities. Int. J. Coal Geol. 229. https://doi.org/10.1016/j.coal.2020.103558.

Buendia, C., Kranjc, K., Fukuda, J., Osako, N.S., Shermanau, Y., Federici, P., 2019. 2019 Refinement to the 2006 IPCC Guidelines for National Greenhouse Gas Inventories Volume 2 Energy Edited by Task Force on National Greenhouse Gas Inventories.

Cater, M., Zorec, M., Marinšek Logar, R., 2014. Methods for improving anaerobic lignocellulosic substrates degradation for enhanced biogas production. Springer Sci. Rev. 2, 51–61. https://doi.org/10.1007/s40362-014-0019-x.

Chabbi, A., Rumpel, C., Grootes, P.M., González-Pérez, J.A., Delaune, R.D., Gonzalez-Vila, F., Nixdorf, B., Hüttl, R.F., 2006. Lignite degradation and mineralization in lignite-containing mine sediment as revealed by 14C activity measurements and molecular analysis. Org. Geochem. 37, 957–976. https://doi.org/10.1016/j.orggeochem.2006.02.002.

Chen, C., Chen, H., Zhang, Y., Thomas, H.R., Frank, M.H., He, Y., Xia, R., 2020. TBtools: an integrative toolkit developed for interactive analyses of big biological data. Mol. Plant 13, 1194–1202. https://doi.org/10.1016/j.molp.2020.06.009.

Ciuk, E., 1991. Historical outline of brown coal exploration, examination and mining in Poland and the role of the State Geological Institute. Geol. Q. 35, 207–220.

Cole, J.J., Prairie, Y.T., 2014. Dissolved CO2 in freshwater systems? Reference Module in Earth Systems and Environmental Sciences. Elsevier https://doi.org/10.1016/b978-0-12-409548-9.09399-4

DeAngelis, K.M., Allgaier, M., Chavarria, Y., Fortney, J.L., Hugenholtz, P., Simmons, B., Sublette, K., Silver, W.L., Hazen, T.C., 2011. Characterization of trapped lignin-degrading microbes in tropical forest soil. PLoS One 6, e19306. https://doi.org/10.1371/journal.pone.0019306.

Detman, A., Bucha, M., Simoneit, B.R.T., Mielecki, D., Piwowarczyk, C., Chojnacka, A., Blaszczyk, M.K., Jedrysek, M.O., Marynowski, L., Sikora, A., 2018. Lignite biodegradation under conditions of acidic molasses fermentation. Int. J. Coal Geol. 196, 274–287. https://doi.org/10.1016/j.coal.2018.07.015.

Dos Santos, E.C., De Mendonça Silva, J.C., Duarte, H.A., 2016. Pyrite oxidation mechanism by oxygen in aqueous medium. J. Phys. Chem. C 120, 2760–2768. https://doi.org/10.1021/acs.jpcc.5b10949.

Eggleston, H.S., Buendia, L., Miwa, K., Ngara, T., Tanabe, K., 2006. IPCC guidelines for national greenhouse gas inventories. Energy, 2006 IPCC Guidelines for National Greenhouse Gas Inventories. Volume 2.

EIA, 2020. Trends and expectations surrounding the outlook for energy markets [WWW document]. URL. www.eia.gov (accessed 12.9.20).

Fabianska, M., 2007. Organic Geochemistry of Brown Coals From the Selected Polish Basin (in Polish). University of Silesia, Katowice.

Fiedler, S., Vepraskas, M.J., Richardson, J.L., 2007. Soil redox potential: importance, field measurements, and observations. Advances in Agronomy. Academic Press, pp. 1–54 https://doi.org/10.1016/S0065-2113(06)94001-2.

Gilewska, M., Otremba, K., 2015. Water reservoirs under construction as a result of the activities of 'Konin' and 'Adamów' brown coal mines. J. Ecol. Eng. 16, 138–143. https://doi.org/10.12911/22998993/60470.

Gläßer, C., Groth, D., Frauendorf, J., 2011. Monitoring of hydrochemical parameters of lignite mining lakes in Central Germany using airborne hyperspectral casi-scanner data. Int. J. Coal Geol. 86, 40–53. https://doi.org/10.1016/j.coal.2011.01.007.

Hammer, Ø., Harper, D.A.T., Ryan, P.D., 2001. Past: paleontological statistics software package for education and data analysis. Palaeontol. Electron. 4, 1–9.

Haney, R.L., Haney, E.B., Smith, D.R., Harmel, R.D., White, M.J., 2018. The soil health tool—theory and initial broad-scale application. Appl. Soil Ecol. 125, 162–168. https://doi.org/10.1016/j.apsoil.2017.07.035.

Hofrichter, M., Fakoussa, R., 2001. Microbial degradation and modification of coal. Lignin, Humic Substances and Coal. Wiley–VCH, pp. 393–427.

Höök, M., 2012. Coal coal and peat peat : global resources peal global resources peat global resources and future supply peal future supply peat future supply. Encyclopedia of Sustainability Science and Technology. Springer, New York, pp. 2173–2194 https://doi.org/10.1007/978-1-4419-0851-3_161.

IEA, 2020. World energy outlook 2020 [WWW Document]. URL. https://www.iea.org/reports/world-energy-outlook-2020.

International Committee for Coal Petrology, 1993. International Handbook of Coal Petrography. 2nd ed. University of Newcastle upon Tyne, England.

Islam, T., Gessesse, A., Garcia-Moyano, A., Murrell, J.C., Øvreås, L., 2020. A novel moderately thermophilic type ib methanotroph isolated from an alkaline thermal spring in the Ethiopian rift valley. Microorganisms 8, 250. https://doi.org/10.3390/microorganisms8020250.

Kanduc, T., Pezdic, J., 2005. Origin and distribution of coalbed gases from the Velenje basin, Slovenia. Geochem. J. 39, 397–409. https://doi.org/10.2343/geochemj.39.397.

Kasinski, J.R., Piwocki, M., Swadowska, E., Ziembinska-Tworzydlo, M., 2010. Lignite of the polish Lowlands miocene: characteristics on a base of selected profiles. Biul. Państw. Inst. Geol. 99–154.

Kezovic, M., 2011. Coal bearing in Kolubara basin (in Serbian with English abstract). J. Public Enterp. Electr. Power Ind. Serbia 154–163.

Khalil, K., Mary, B., Renault, P., 2004. Nitrous oxide production by nitrification and denitrification in soil aggregates as affected by O2 concentration. Soil Biol. Biochem. 36, 687–699. https://doi.org/10.1016/j.soilbio.2004.01.004.

Kholod, N., Evans, M., Pilcher, R.C., Roshchanka, V., Ruiz, F., Coté, M., Collings, R., 2020. Global methane emissions from coal mining to continue growing even with declining coal production. J. Clean. Prod. 256, 120489. https://doi.org/10.1016/j.jclepro.2020.120489.

Knoema, 2020. Production of lignite coal [WWW Document]. World data atlas. URL. https://knoema.com/atlas/topics/Energy/Coal/Production-of-lignite-coal (accessed 3.23.21).

Lian, Y., Yang, Y., Guo, J., Wang, Y., Li, X., Fang, Y., Gan, L., Xu, M., 2016. Electron acceptor redox potential globally regulates transcriptomic profiling in shewanella decolorationis S12. Sci. Rep. 6, 1–9. https://doi.org/10.1038/srep31143.

Liber-Makowska, E., 2013. Geothermal conditions of the Turoszów Basin (in Polish). Tech. Poszuk. Geol. Geoterm. Zrównowazony Rozw. 1, 135–142.

Liu, J., Peach, C.J., Spiers, C.J., 2016. Anisotropic swelling behaviour of coal matrix cubes exposed to water vapour: effects of relative humidity and sample size. Int. J. Coal Geol. 167, 119–135. https://doi.org/10.1016/j.coal.2016.09.011.

Liu, B., Vrabec, M., Markic, M., Püttmann, W., 2019. Reconstruction of paleobotanical and paleoenvironmental changes in the pliocene Velenje Basin, Slovenia, by molecular and stable isotope analysis of lignites. Int. J. Coal Geol. 206, 31–45. https://doi.org/10.1016/j.coal.2019.03.006.

Liu, H., Wrage-Mönnig, N., Lennartz, B., 2020. Rewetting strategies to reduce nitrous oxide emissions from European peatlands. Commun. Earth Environ. 1, 1–7. https://doi.org/10.1038/s43247-020-00017-2.

Martin, F., Ebel, B., Rojas, C., Gervais, P., Cayot, N., Cacho, R., 2013. Redox potential: monitoring and role in development of aroma compounds, rheological properties and survival of oxygen sensitive strains during the manufacture of fermented dairy products. Lactic Acid Bacteria - R & D for Food, Health and Livestock Purposes. InTech https://doi.org/10.5772/51137.

Mastej, W., Bartus, T., Rydlewski, J., 2015. Analysis of lithofacies cyclicity in the miocene coal complex of the Bełchatów lignite deposit, south-Central Poland. Geologos 21, 285–302. https://doi.org/10.1515/logos-2015-0021.

Meissner, K., 1962. Wlasnosci geotechniczne skal nadkladu w Koninskim Zaglebiu Wegla Brunatnego, Przeglad Geologiczny.

Myhre, G., Shindell, D., Bréon, F., Collins, W., Fuglestvedt, J., Huang, J., Koch, D., Lamarque, J., Lee, D., Mendoza, B., Nakajima, T., Robock, A., Stephens, G., Takemura, T., Zhan, H., 2013. Anthropogenic and natural radiative forcing. Climate Change 2013: The Physical Science Basis. Contribution of Working Group I to the Fifth Assessment Report of the Intergovernmental Panel on Climate Change. Cambridge Univ. Press, Cambridge, United Kingdom New York, NY, USA, pp. 659–740.

Nyga-Lukaszewska, H., Aruga, K., Stala-Szlugaj, K., 2020. Energy security of Poland and coal supply: price analysis. Sustainability 12, 2541. https://doi.org/10.3390/su12062541.

Otto, A., Simoneit, B.R.T., 2001. Chemosystematics and diagenesis of terpenoids in fossil conifer species and sediment from the Eocene Zeitz formation, Saxony, Germany. Geochim. Cosmochim. Acta 65, 3505–3527. https://doi.org/10.1016/S0016-7037(01)00693-7.

Pawelec, S., Bielowicz, B., 2016. Petrographic composition of lignite from the Szczerców deposit, Polish Lowlands. Contemp. Trends Geosci. 5, 92–103. https://doi.org/10.1515/ctg-2016-0007.

Piwocki, M., 1992. Extent and correlations of main groups of the tertiary lignite seams on polish platform area. Prz. Geol. 40, 281–286.

Polish Geological Institute, 2020. Mineral resources of Poland [WWW document]. Website. URL. http://geoportal.pgi.gov.pl/surowce/energetyczne/wegiel_brunatny/2019 (accessed 3.22.21).

Prem, E.M., Mutschlechner, M., Stres, B., Illmer, P., Wagner, A.O., 2021. Lignin intermediates lead to phenyl acid formation and microbial community shifts in meso- and thermophilic batch reactors. Biotechnol. Biofuels 14, 1–23. https://doi.org/10.1186/s13068-020-01855-0.

Public Enterprize Electric Power Industry of Serbia, 2020. Production of coal [WWW document]. URL. http://www.eps.rs/eng/poslovanje-ugalj (accessed 3.22.21).

Pytlak, A., Stepniewska, Z., Kuzniar, A., Szafranek-Nakonieczna, A., Wolinska, A., Banach, A., 2014. Potential for aerobic methane oxidation in carboniferous coal measures. Geomicrobiol J. 31, 737–747. https://doi.org/10.1080/01490451.2014.889783.

Pytlak, A., Sujak, A., Szafranek-Nakonieczna, A., Grzadziel, J., Banach, A., Goraj, W., Galazka, A., Gruszecki, W.I., Stepniewska, Z., 2020a. Water-induced molecular changes of hard coals and lignites. Int. J. Coal Geol. 224, 103481. https://doi.org/10.1016/j.coal.2020.103481.

Pytlak, A., Szafranek-Nakonieczna, A., Sujak, A., Grzadziel, J., Polakowski, C., Kuzniar, A., Proc, K., Kubaczynski, A., Goraj, W., Galazka, A., Gruszecki, W.I., Bieganowski, A., Stepniewska, Z., 2020b. Stimulation of methanogenesis in bituminous coal from the upper silesian coal basin. Int. J. Coal Geol. 231. https://doi.org/10.1016/j.coal.2020.103609.

Pytlak, A., Sparkes, R., Goraj, W., Szafranek-Nakonieczna, A., Banach, A., Akmetkaliyeva, S., Slowakiewicz, M., 2021. Methanotroph-derived bacteriohopanepolyol signatures in sediments covering miocene brown coal deposits. Int. J. Coal Geol. 103759. https://doi.org/10.1016/j.coal.2021.103759.

Robbins, S.J., Evans, P.N., Esterle, J.S., Golding, S.D., Tyson, G.W., 2016. The effect of coal rank on biogenic methane potential and microbial composition. Int. J. Coal Geol. 154–155, 205–212. https://doi.org/10.1016/j.coal.2016.01.001.

Saunois, M., Stavert, A.R., Poulter, B., Bousquet, P., Canadell, J.G., Jackson, R.B., Raymond, P.A., Dlugokencky, E.J., Houweling, S., Patra, P.K., Ciais, P., Arora, V.K., Bastviken, D., Bergamaschi, P., Blake, D.R., Brailsford, G., Bruhwiler, L., Carlson, K.M., Carrol, M., Castaldi, S., Chandra, N., Crevoisier, C., Crill, P.M., Covey, K., Curry, C.L., Etiope, G., Frankenberg, C., Gedney, N., Hegglin, M.I., Höglund-Isaksson, L., Hugelius, G., Ishizawa, M., Ito, A., Janssens-Maenhout, G., Jensen, K.M., Joos, F., Kleinen, T., Krummel, P.B., Langenfelds, R.L., Laruelle, G.G., Liu, L., MacHida, T., Maksyutov, S., McDonald, K.C., McNorton, J., Miller, P.A., Melton, J.R., Morino, I., Müller, J., Murguia-Flores, F., Naik, V., Niwa, Y., Noce, S., O'Doherty, S., Parker, R.J., Peng, C., Peng, S., Peters, G.P., Prigent, C., Prinn, R., Ramonet, M., Regnier, P., Riley, W.J., Rosentreter, J.A., Segers, A., Simpson, I.J., Shi, H., Smith, S.J., Paul Steele, L., Thornton, B.F., Tian, H., Tohjima, Y., Tubiello, F.N., Tsuruta, A., Viovy, N., Voulgarakis, A., Weber, T.S., Van Weele, M., Van Der Werf, G.R., Weiss, R.F., Worthy, D., Wunch, D., Yin, Y., Yoshida, Y., Zhang, W., Zhang, Z., Zhao, Y., Zheng, B., Zhu, Q., Zhu, Q., Zhuang, Q., 2020. The global methane budget 2000-2017. Earth Syst. Sci. Data 12, 1561–1623. https://doi.org/10.5194/essd-12-1561-2020.

Schlesinger, W.H., 1997. Biogeochemistry: An Analysis of Global Change. 2nd ed. Academic Press, San Diego.

Sheehan, R., McCarver, A.C., Isom, C.E., Karr, E.A., Lessner, D.J., 2015. The methanosarcina acetivorans thioredoxin system activates DNA binding of the redox-sensitive transcriptional regulator MsvR. J. Ind. Microbiol. Biotechnol. 42, 965–969. https://doi.org/10.1007/s10295-015-1592-y.

Sikora, A., Detman, A., Chojnacka, A., Blaszczyk, M.K., 2017. Anaerobic digestion: I. A common process ensuring energy flow and the circulation of matter in ecosystems. II. A tool for the production of gaseous biofuels. Fermentation Processes. InTech https://doi.org/10.5772/64645.

Stepniewska, Z., Pytlak, A., 2008. Methanotrophic activity of coalbed rocks from 'Bogdanka' coal mine (south-east Poland). Arch. Environ. Prot. 34, 183–191.

Stepniewska, Z., Pytlak, A., Kuzniar, A., 2013. Methanotrophic activity in carboniferous coalbed rocks. Int. J. Coal Geol. 106, 1–10. https://doi.org/10.1016/j.coal.2013.01.003.

Stepniewska, Z., Pytlak, A., Kuzniar, A., 2014. Distribution of the methanotrophic bacteria in the Western part of the Upper Silesian Coal Basin (Borynia-Zofiówka and Budryk coal mines). Int. J. Coal Geol. https://doi.org/10.1016/j.coal.2014.05.003.

Strapoc, D., Mastalerz, M., Dawson, K., Macalady, J., Callaghan, A.V., Wawrik, B., Turich, C., Ashby, M., 2011. Biogeochemistry of microbial coal-bed methane. Annu. Rev. Earth Planet. Sci. 39, 617–656. https://doi.org/10.1146/annurev-earth-040610-133343.

Szafranek-Nakonieczna, A., Zheng, Y., Slowakiewicz, M., Pytlak, A., Polakowski, C., Kubaczynski, A., Bieganowski, A., Banach, A., Wolinska, A., Stepniewska, Z., 2018. Methanogenic potential of lignites in Poland. Int. J. Coal Geol. 196, 201–210. https://doi.org/10.1016/j.coal.2018.07.010.

Wang, Z.P., DeLaune, R.D., Patrick, W.H., Masscheleyn, P.H., 1993. Soil redox and pH effects on methane production in a flooded Rice soil. Soil Sci. Soc. Am. J. 57, 382–385. https://doi.org/10.2136/sssaj1993.03615995005700020016x.

Widera, M., 2012. Macroscopic lithotype characterisation of the 1st middle-polish (1st Lusatian) lignite seam in the miocene of Central Poland. Geologos 18, 1–11. https://doi.org/10.2478/v10118-012-0001-5.

Widera, M., 2016. Characteristics and origin of deformation structures within lignite seams – a case study from polish opencast mines. Geol. Q. 60, 179–189. https://doi.org/10.7306/gq.1268.

Widera, M., 2016b. An overview of lithotype associations of miocene lignite seams exploited in Poland. Geologos 22, 213–225. https://doi.org/10.1515/logos-2016-0022.

Widera, M., Jachna-Filipczuk, G., Kozula, R., Mazurek, S., 2007. From peat bog to lignite seam: a new method to calculate the consolidation coefficient of lignite seams, wielkopolska region in Central Poland. Int. J. Earth Sci. 96, 947–955. https://doi.org/10.1007/s00531-006-0137-z.

Yu, K., Faulkner, S.P., Patrick, W.H., 2006. Redox potential characterization and soil greenhouse gas concentration across a hydrological gradient in a gulf coast forest. Chemosphere 62, 905–914. https://doi.org/10.1016/j.chemosphere.2005.05.033.

Životic, D., Stojanovic, K., Gržetic, I., Jovancicevic, B., Cvetkovic, O., Šajnovic, A., Simic, V., Stojakovic, R., Scheeder, G., 2013. Petrological and geochemical composition of lignite from the D field, kolubara basin (Serbia). Int. J. Coal Geol. 111, 5–22. https://doi.org/10.1016/j.coal.2012.10.014.